Spectral Analysis of Unevenly Spaced Data: Models and Application in Heart Rate Variability

Martin Bachler

Center for Health and Bioresources, AIT Austrian Institute of Technology, Giefinggasse 4, 1210 Vienna, Austria; *martin.bachler@ait.ac.at*

SNE 27(4), 2017, 183-190, DOI: 10.11128/sne.27.tn.10393
Received: November 10, 2017, Revised: December 10, 2017, Accepted: December 15, 2017
SNE - Simulation Notes Europe, ARGESIM Publisher Vienna, ISSN Print 2305-9974, Online 2306-0271, www.sne-journal.org

Abstract. Heart rate variability (HRV) is the temporal variation of the interval between consecutive heartbeats. It can be analyzed by numerous methods, including spectral analysis. However, HRV time series naturally consist of unevenly spaced data. Several methods emerged to counteract this problem, usually yielding different results. Therefore, in this work three spectral analysis methods were investigated: the Welch, Lomb-Scargle, and Burg method. Their properties were analyzed by theoretical considerations and verified in simulations. Using an oscillator network model with the integral pulse frequency modulation model, artificial HRV time series were generated. Their power spectral densities and their dominant frequencies were evaluated and compared to the nominal values of the simulated time series. The results of these experiments and the theoretical considerations suggest that the Lomb-Scargle method is the most exact in reproducing power spectral densities and dominant frequencies of unevenly spaced HRV data.

Introduction

Heart rate variability (HRV) is the temporal variation of the interval between consecutive heartbeats. It reflects the ability of an organism to change the frequency of the cardiac rhythm on a beat-to-beat basis.

The heart rhythm is controlled via the autonomic nervous system, whereby its two branches, the sympathetic and the parasympathetic, produce acceleration or deceleration. The sympathetic nervous system has an activating function and causes an increase in the heart rate, the parasympathetic nervous system leads to an inhibition of the activity and therefore a decrease in the heart rate [1].

The higher the heart rate variability, the faster and more flexible the organism can adapt to internal and external influences, by optimizing the interplay of the sympathetic and parasympathetic nervous system. Physical or psychological stress usually results in an increase in the heart rate, which then recedes during relief and relaxation. Under chronic stress, however, this adaptability is restricted and consequently the HRV is reduced due to the constantly high tension [2]. The regulatory system of the heart rate has several highly interconnected in- and outputs, which lead to complex irregularity in the resulting heart rate. Therefore, it is reasonable to hypothesize that a defect in the regulatory system leads to a decreased irregularity of the heart rate. Thus, the analysis of the HRV strives to quantify the amount of variability and irregularity.

In diagnostic terms, HRV is not a clinical parameter or biomarker, but an umbrella term. It can be quantified from a series of RR intervals (i.e., the series of beat-to-beat intervals) by numerous parameters in three categories:

- By statistical parameters in the time-domain: the beat-to-beat heart rate is interpreted as a time series and is described using common methods of time series analysis [1].
- By spectral analysis in the frequency-domain: the beat-to-beat heart rate is regarded as a time-dependent function and transformed into the frequency-domain. The power spectral density of certain, standardized frequency bands reflects various physiological processes [1].
- By non-linear analysis methods: This collective term encompasses all methods that attempt to

quantify the complex dynamics of the physiological interactions of the cardiac, circulatory and nervous system to control the heart rate. Methods from the field of chaos theory may be applied to determine short-term variability (Poincaré plot) or the degree of irregularity (entropy analysis) [3, 4].

The analysis of the power spectral density (PSD) provides information on how power distributes as a function of frequency. The power of certain frequency bands can be linked to sympathetic and parasympathetic activity, respiratory sinus arrhythmia, circadian rhythms, and further physiologic influences on the HRV. The Guidelines on Heart Rate Variability distinguish between the total power of the whole spectrum and the spectral power of four separated frequency bands, usually determined in ms^2, as summarized in table 1.

Name	Description	Frequency range
TP	Total Power	0 - 0.4 Hz
ULF	Ultra low frequency	0 - 0.003 Hz
VLF	Very low frequency	0.003 - 0.04 Hz
LF	Low frequency	0.04 - 0.15 Hz
HF	High frequency	0.15 - 0.4 Hz

Table 1: Summary of frequency-domain measures of HRV.

The applicability of these measures depends on the duration of the recording. Power in the ultra low frequency (ULF) and very low frequency (VLF) ranges can only be determined in long-term 24h recordings, since their cycle times $(1/f)$ exceed 5 minutes. On the other hand, the power in the low (LF) and high (HF) frequency ranges can be calculated in short- and long-term recordings alike. However, since the heart rate modulations during long-term recordings exhibit lower stability, LF and HF become less easily interpretable. The total power (TP) is applicable in short- and long-term recordings without constraint [1]. Figure 1 shows an example of a PSD analysis with frequency bands.

The estimation of the PSD itself is not a trivial process, since methods for spectral analysis usually require evenly sampled discrete time series. This is not the case for a series of RR intervals, since the heartbeats form a discrete event series following a stochastic process. Several methods emerged to counteract this problem, essentially based on two approaches. *Non-parametric* methods do not assume a functional form of the PSD a priori, while for *parametric* methods, assumptions are made for the signal which lead to a parametric, functional form of the PSD. In the latter case, parameters for the resulting model have to be determined.

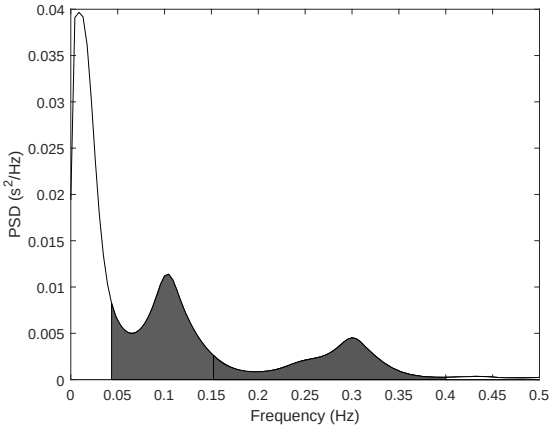

Figure 1: Example of a power spectral density estimate of a 5 minute recording. The blue area marks the LF, the red area the HF component of the spectrum.

Both approaches have advantages and disadvantages. Therefore, in this work, popular models for the PSD estimation of HRV time series are investigated by theoretical considerations and application of the methods to simulated data.

1 Methods

In the first part of this section, the non-parametric and parametric PSD estimation methods commonly used in HRV analysis are described. In the second part, methods to simulate artificial HRV time series are presented. The PSD estimation methods are then applied to the simulated time series and their results compared to the nominal values of the simulation.

1.1 Non-Parametric PSD Methods

Non-parametric methods are based on the fast Fourier transform. Due to finite data length the definition of the PSD is modified to an empirical version based on the discrete-time Fourier transform (DTFT) and thus an estimate. This estimate is referred to as a periodogram and is calculated for a signal $y(t)$ as follows:

$$\hat{S}_{XX}(\omega) = \frac{1}{N}\left|\sum_{t=1}^{N} y(t)\, e^{-i\omega t}\right|^2. \quad (1)$$

However, this direct DTFT approach has high variance and is not consistent [5]. Furthermore, these estimates exhibit distortions due to spectral leakage caused by the windowing effect of finite data lengths, which may cause a superposition of weak parts of the signal [2]. Therefore, methods such as the Welch method were developed to reduce variance and spectral leakage at the expense of the resolution [5].

Welch Method In the Welch method, the data points are divided into segments that can overlap. The data points of each segment are weighted with a window function before calculating the periodogram. In order to obtain the estimated value of the PSD, the periodograms of the individual segments are averaged. This averaging should lead to a reduction in variance [6].

In order to create an evenly sampled discrete time series, the RR intervals in this work are first interpolated at 7 Hz and subsequently evaluated using the Welch method with adjacent segments overlapping at 50% and a Hamming window function [7].

Lomb-Scargle Method An advancement of the classical periodogram is the variant of Lomb and Scargle [8, 9], whose great advantage is the applicability to stochastic, irregularly sampled data. It was originally developed for application in astronomical research, where observation periods are limited and irregular due to planetary constellations and weather influences. It is able to find weak periodic signals in otherwise random, unevenly sampled data. Studies show that the Lomb-Scargle periodogram reduces possible distortions or erroneous results that can result from any form of interpolation [10].

Consider x_k being the RR intervals and t_k derived from the discrete event series of R peaks, where $k = 1,\ldots,N$. The Lomb-Scargle periodogram is defined by [8] as

$$P_{LS}(\omega) = \frac{1}{2\sigma^2}\left\{\frac{\left[\sum_{k=1}^{N}(x_k-\bar{x})\cos(\omega(t_k-\tau))\right]^2}{\sum_{k=1}^{N}\cos^2(\omega(t_k-\tau))} + \frac{\left[\sum_{k=1}^{N}(x_k-\bar{x})\sin(\omega(t_k-\tau))\right]^2}{\sum_{k=1}^{N}\sin^2(\omega(t_k-\tau))}\right\}, \quad (2)$$

where $\bar{x}$ is the mean and σ^2 the variance of x. For every angular frequency $\omega = 2\pi f$ a time offset τ is chosen as

$$\tan(2\omega\tau) = \frac{\sum_{k=1}^{N}\sin(2\omega t_k)}{\sum_{k=1}^{N}\cos(2\omega t_k)}. \quad (3)$$

The time offset τ guarantees the time invariance of P_{LS}, since every shift of t_k results in an equivalent shift in the offset.

1.2 Parametric PSD Methods

Non-parametric methods do not assume any conditions for the signal except for stationarity. In the case of a parametric or model-based approach for spectral estimation, the signal is given a certain functional form and thus a model is created. The parameters of the model must be determined.

Burg Method Despite the existence of a wide variety of parametric methods, the most wide spread for analysis of HRV models the RR intervals as an autoregressive process of the form

$$y(t) = c + \sum_{i=1}^{p}\phi_i y(t-i) + \varepsilon_t, \quad (4)$$

where c is a constant, ε_t a white-noise error term, and ϕ_i represents the model parameters. The order p of the model influences its properties: the lower the order, the smoother the resulting PSD function. Previous studies suggest that an order of $p = 16$ is best suited for application in HRV analysis [11, 2]. Finally, the Burg method, whose algorithm minimizes predefined forward and backward prediction errors, is used to estimate the model parameters ϕ_i [12].

The three methods for PSD estimation are compared in figure 2. Due to the segmentation of the input series, the Welch method shows fewer resulting data points than the other two methods. The Lomb-Scargle method exhibits more distinct peaks and valleys with maximum values about twice the height of the other two methods. However, the integral of the power in the LF and HF band is comparable especially to the Burg method. The Burg method, due to the underlying autoregressive model, shows the smoothest shape.

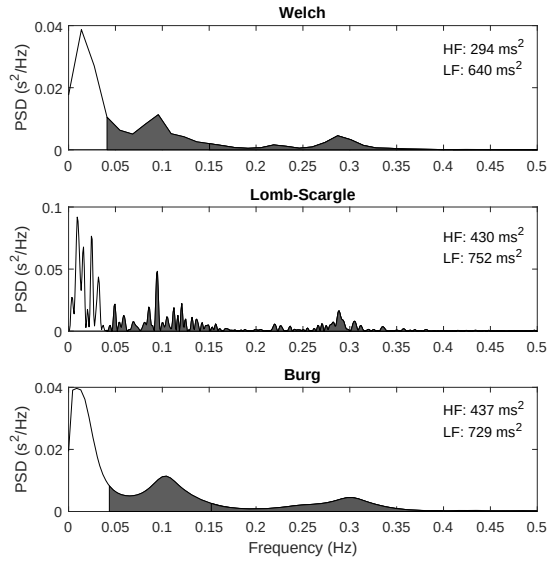

Figure 2: Comparison of the three PSD estimation methods of the same HRV time series: Welch (50% overlap, Hamming window), Lomb-Scargle, and Burg (order 16).

$$s_{HF}(t) = \sum_{i=1}^{3} a_{HFi} \cdot \sin(2\pi f_{HFi} t) \quad (7)$$

$$m(t) = HR + s_{VLF} + s_{LF} + s_{HF}, \quad (8)$$

where HR is a constant offset representing the average heart rate (HR).

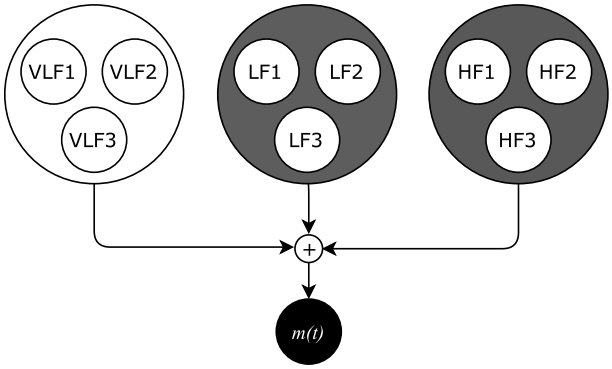

Figure 3: Network of oscillators to simulate the cardiac control system $m(t)$.

1.3 Simulation of HRV Time Series

Different frequency bands in the HRV time series reflect different physiological feedback mechanisms. In order to generate artificial HRV time series it is possible to reversely approximate this connection. In this work, the following two models were coupled in order to simulate unevenly spaced HRV data.

Oscillator Network Model Based on the work of Brennan et al. [13], an interconnected network of sine oscillators is created to simulate the cardiac control system, as shown in figure 3. To create a more realistic frequency distribution, each frequency band (VLF, LF, and HF) is simulated by three sub-oscillators. Thereby, each sub-oscillator is determined by its fundamental frequency f_i (randomly chosen in the respective frequency range) and its amplitude a_i, randomly chosen in the range of $[20,40]ms$. Finally, the cardiac control system $m(t)$ is given by

$$s_{VLF}(t) = \sum_{i=1}^{3} a_{VLFi} \cdot \sin(2\pi f_{VLFi} t) \quad (5)$$

$$s_{LF}(t) = \sum_{i=1}^{3} a_{LFi} \cdot \sin(2\pi f_{LFi} t) \quad (6)$$

Integral Pulse Frequency Modulation Model Since equation 7 produces a continuous model of the cardiac control system, another step is required to generate unevenly spaced HRV data. In this step, the integral pulse frequency modulation (IPFM) model is applied [14]. It generates the occurrence times of heartbeats by integrating the input signal $m(t)$ until it reaches unity. This point in time is then considered as occurrence of one heartbeat, and the integrator is reset to zero. It is represented as

$$1 = \int_{t_k}^{t_{k+1}} m(t)dt, \quad (9)$$

where t_k denotes the occurrence times of heartbeats. In this work, equation 9 was solved numerically for $t \in [0,300]$ seconds. This duration corresponds to HRV measurements of 5 minutes and follows the Guidelines on Heart Rate Variability [1]. Finally, the HRV time series consists of the intervals between consecutive heartbeats, the RR intervals, and is therefore derived from the t_k series as

$$RR_k = t_{k+1} - t_k. \quad (10)$$

1.4 Model Comparison

Since the HRV data in this work is generated artificially, it is possible to determine their nominal values and compare them to the results of the investigated methods. This comparison will focus on two features of the HRV time series: (1) the power spectral density and (2) the most dominant frequency. Both features will be independently evaluated for the LF and HF component.

Power Spectral Density The PSD of a given continuous signal $x(t)$ in the time domain is given by

$$P = \lim_{T\to\infty} \frac{1}{2T} \int_{-T}^{T} |x(t)|^2 dt. \tag{11}$$

For a signal of finite duration T, equation 11 reduces to the variance of the signal. Since the frequency components are generated separately in the oscillator model, the nominal values for LF and HF power p_{LF} and p_{HF} are calculated by

$$P_{LF} = \mathrm{Var}(s_{LF}), \text{ and} \tag{12}$$
$$P_{HF} = \mathrm{Var}(s_{HF}). \tag{13}$$

As comparison, the band limited PSD of the Welch, Lomb-Scargle, and Burg method will be calculated by

$$\hat{P} = 2 \int_{f_1}^{f_2} \hat{S}_{XX}(2\pi f) df \tag{14}$$

from their respective PSD estimations $\hat{S}_{XX}$ and in the frequency ranges $[f_1, f_2]$ according to table 1.

Dominant Frequency Again, the fact that the frequency components are generated separately is used to obtain nominal values for the model comparison. For the component s_{LF} (and likewise for s_{HF}), the dominant frequency f_d is determined by the amplitude:

$$i = \underset{i}{\mathrm{argmax}}(a_{LFi}), \tag{15}$$
$$f_d = f_{LFi}. \tag{16}$$

The comparative values from the PSD methods are obtained from the PSD estimates $\hat{S}_{XX}$ by

$$\hat{f}_d = \underset{f\in[f_1,f_2]}{\mathrm{argmax}}(\hat{S}_{XX}(2\pi f)). \tag{17}$$

2 Results

One thousand simulation runs of the HRV model were performed to gather nominal values and approximations by the Welch, the Lomb-Scargle, and the Burg PSD estimation methods. Their results are reported in this section.

2.1 Power Spectral Density

Figure 4 summarizes the differences between the PSD evaluated by the three methods under investigation and the nominal values as boxplots. The same results are aggregated in table 2 as mean (standard deviation). While in the LF band, the Welch method shows the best result regarding the mean and median differences, it also shows the worst in the HF band. In contrast, the Lomb-Scargle method exhibits the worst result regarding the mean and median differences in the LF range. However, its scattering is by far the lowest in all tested cases, suggesting a higher consistency compared to the other methods.

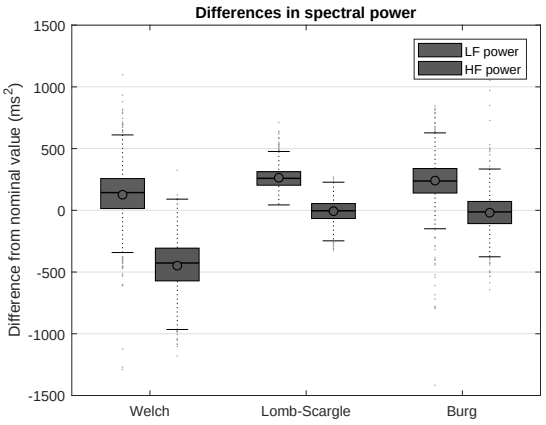

Figure 4: Deviation of the power spectral density approximations from the nominal values in the low- and high frequency (LF and HF) range.

Figure 5 shows the individual differences of all simulation runs as a function of the nominal values. It allows the interpretation of the results regarding systematic errors. Again, the lower dispersion of the Lomb-Scargle method is clearly visible. Furthermore, all methods display a dependency on the nominal values: the higher the nominal values, the higher the dispersion of the differences. Lastly, trends are visible in the evaluation of the LF range by the Lomb-Scargle method and

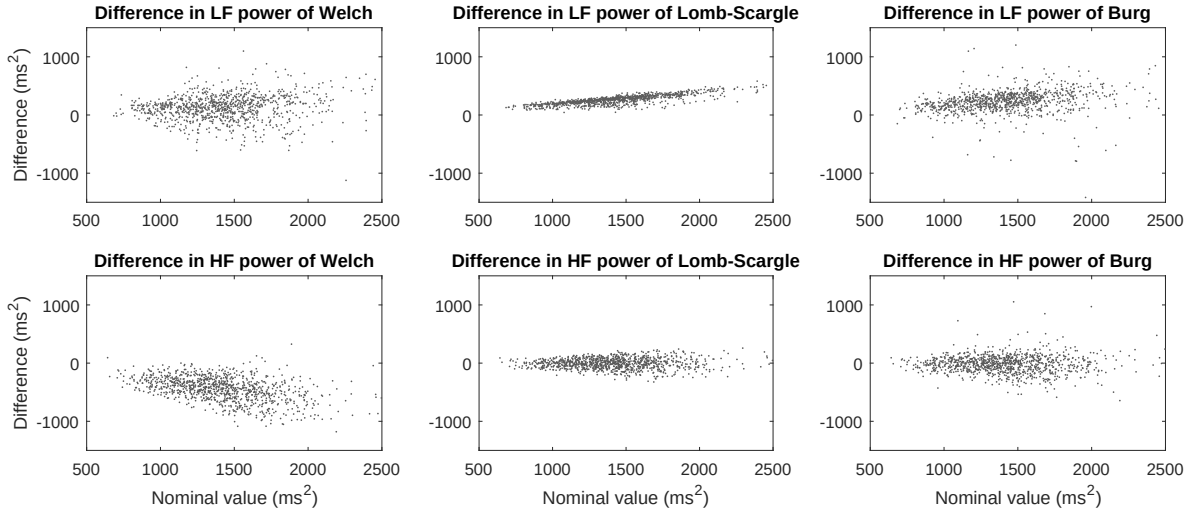

Figure 5: Deviation of the power spectral density approximations from the nominal values, shown as a function of the nominal values and separated by method and frequency range.

Power Spectral Density	LF (ms^2)	HF (ms^2)
Welch	126 (232)	-448 (214)
Lomb-Scargle	264 (88)	-7 (93)
Burg	241 (281)	-19 (156)

Table 2: Deviation of the power spectral density approximations from the nominal values in the low- and high frequency (LF and HF) range, stated as mean (Standard deviation).

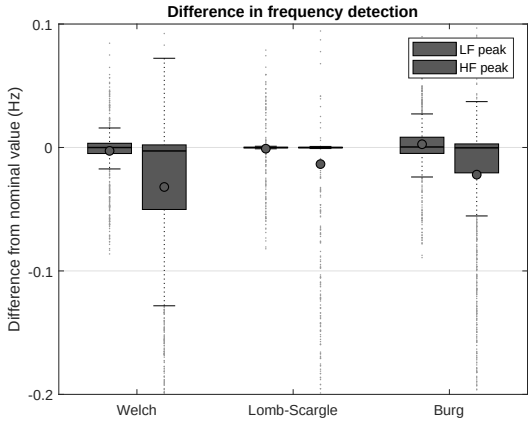

Figure 6: Deviation of the detected dominant frequency from the nominal values in the low- and high frequency (LF and HF) range.

the HF range by the Welch method. In these cases, apparently the differences of the results and nominal values depend on the actual power of the respective frequency band.

2.2 Dominant Frequency

Figure 6 reports the deviation of the detected dominant frequencies from the nominal values. Since the results are not normally distributed, table 3 summarizes them as median [1st quartile, 3rd quartile]. In contrast to the results of the PSD, the Lomb-Scargle method outperforms the other methods regarding the dominant frequency in all cases. Again, a low scattering suggests a high consistency of this method.

Figure 7 reports the individual results as a function of the nominal values. All results exhibit the interesting pattern that differences are positive for low frequency values, and negative for high frequency values. This points out the systematic error that measurement results are too high for low frequencies, and too low for high frequencies. In other words, all three methods exhibit a trend towards the center of the frequency range when looking for the most dominant frequency. Apart from this common systematic error, the figure mirrors the results of figure 6 and table 3 regarding the dispersion of the differences. Finally, a reduction of frequency resolution in the Welch method becomes obvious as recurring pattern around the zero difference.

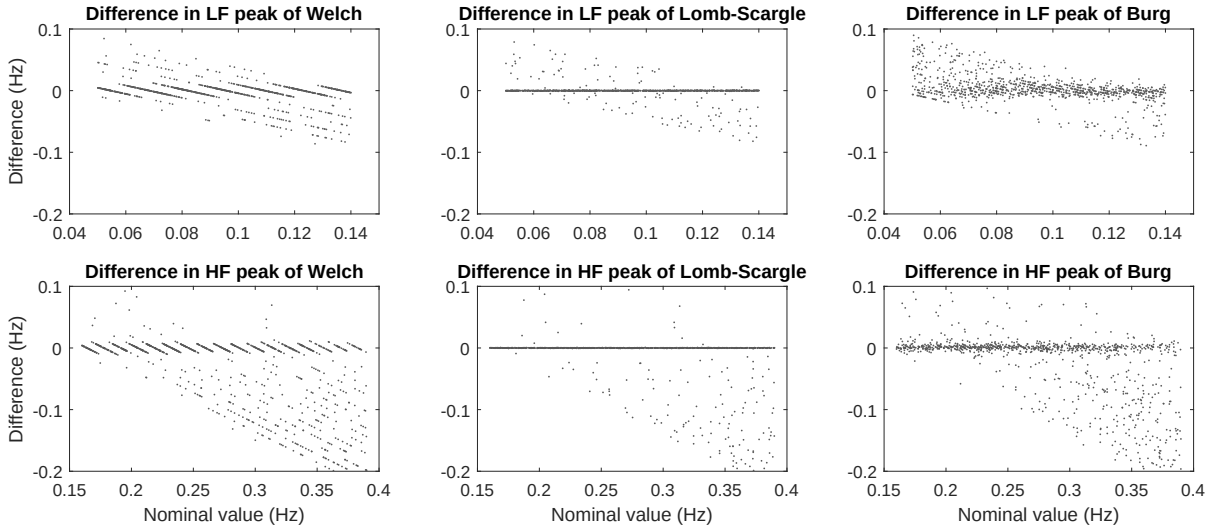

Figure 7: Deviation of the detected dominant frequency peak from the nominal values, shown as a function of the nominal values and separated by method and frequency range. A positive difference results from measurement values higher than the nominal values.

Dominant Freq.	LF (mHz)	HF (mHz)
Welch	0.0 [-4.9, 3.4]	-2.8 [-50.2, 2.1]
Lomb-Scargle	0.0 [-0.3, 0.2]	-0.1 [-0.3, 0.2]
Burg	0.4 [-4.8, 8.3]	-0.3 [-20.6 2.9]

Table 3: Deviation of the detected dominant frequency from the nominal values in the low- and high frequency (LF and HF) range. Since the data is not normally distributed, they are stated as median [1st quartile, 3rd quartile].

3 Discussion

From a clinical point of view, the calculation of the HRV can be used to assess the state of the autonomous nervous system to evaluate e.g. stress, depression, or brain damage [2]. Regarding cardiovascular diseases, HRV analysis aids in the diagnosis and risk stratification of numerous pathologies. Alterations in certain HRV measures during or after myocardial infarction, in congestive heart failure, or in diabetic neuropathy have been linked to increased mortality [1].

While the relationship between the frequency components HF, LF, and VLF and the activity of the nervous system as well as other regulatory mechanisms is undoubted [2], the selection of the proper method to estimate the PSD and their parameters (for parametric methods) remains controversial. Studies showed that the power calculated in the respective frequency bands varies significantly between methods [15].

The Welch method requires evenly sampled data points, which necessitates resampling of the time series. The choice of the resampling method and frequency therefore will influence the PSD estimate. Besides, due to windowing and averaging, the Welch method suffers from a loss in frequency resolution. However, since HRV is usually quantified using the standardized and rather broad frequency bands, this might not be an issue. Furthermore, the windowing and averaging leads to a better statistical stability regarding outliers. Therefore, a small amount of artifacts or ectopic beats in the interval time series is tolerable. [1, 2, 15]

While the Burg methods differs from the Welch method in being parametric instead of non-parametric, they share several advantages and disadvantages. It requires the choice of an order, which affects the result. However, several studies investigated this topic and reached the conclusion, that an order of 16 is generally acceptable in HRV analysis [11, 2]. Similar to the Welch method, the autoregressive model leads to a smoothing effect, limiting the frequency resolution but allowing for some outliers in the time series [15].

The Lomb-Scargle method can be considered the most exact method, since there is no need for resampling (and thus, an alteration of the input data itself)

nor for the choice of parameters. However, it is rarely used in medical studies, probably for the lack of being mentioned in guidelines [1] or thorough reviews [2]. Furthermore, due to the lack of any smoothing, outliers may easily disrupt the PSD estimate, especially the HF component. Therefore, the Lomb-Scargle method requires the most thorough filtering of RR intervals.

Apart from the theoretic analysis, the PSD estimation methods investigated in this work were applied to artificially simulated HRV data with known properties. The results of these model comparisons clearly point towards the Lomb-Scargle method as the most exact method. It showed the best capability to consistently reproduce the power spectral density as well as the accurate detection of the most dominant frequencies. The findings of these simulations are in line with the theoretical considerations.

4 Conclusion

In this work, three methods for spectral analysis of HRV time series were investigated theoretically and using simulated HRV data. The experimental results as well as the theoretical considerations suggest that the Lomb-Scargle method is the most exact. However, it must be assumed that it is also the most vulnerable to outliers in the HRV time series. Therefore, the Lomb-Scargle PSD is only recommended after thorough filtering of the RR intervals, if an error-free time series can be assumed. The effects of outliers on PSD estimation methods therefore will be investigated in future works.

References

[1] American Heart Association Inc; European Society of Cardiology. Guidelines – Heart rate variability. *European Heart Journal*. 1996;17:354–381.

[2] Rajendra Acharya U, Paul Joseph K, Kannathal N, Lim C, Suri J. Heart rate variability: a review. *Medical and Biological Engineering and Computing*. 2006; 44:1031–1051.

[3] Bachler M, Hörtenhuber M, Mayer C, Holzinger A, Wassertheurer S. Entropy-Based Data Mining on the Example of Cardiac Arrhythmia Suppression. In: *Brain Informatics and Health*, edited by Ślęzak D, Tan AH, Peters J, Schwabe L, vol. 8609 of *Lecture Notes in Computer Science*, pp. 574–585. Springer International Publishing. 2014;ISBN: 978-3-319-09890-6 (Print) 978-3-319-09891-3 (Online).

[4] Hagmair S, Bachler M, Wassertheurer S, Mayer C. Nonlinear Methods in Heart Rate Variability: Can they Distinguish between Nonpathological and Pathological Subjects? *SNE Simulation Notes Europe*. 2015; 25(3–4):145–150.

[5] Stoica P, Moses RL, et al. *Spectral analysis of signals*, vol. 452. Pearson Prentice Hall Upper Saddle River, NJ. 2005.

[6] Welch P. The use of fast Fourier transform for the estimation of power spectra: a method based on time averaging over short, modified periodograms. *IEEE Transactions on audio and electroacoustics*. 1967; 15(2):70–73.

[7] Clifford G, Tarassenko L. Quantifying errors in spectral estimates of HRV due to beat replacement and resampling. *Biomedical Engineering, IEEE Transactions on*. 2005;52(4):630–638.

[8] Lomb N. Least-squares frequency analysis of unequally spaced data. *Astrophysics and space science*. 1976; 39(2):447–462.

[9] Scargle JD. Studies in astronomical time series analysis. II-Statistical aspects of spectral analysis of unevenly spaced data. *The Astrophysical Journal*. 1982; 263:835–853.

[10] Ruf T. The Lomb-Scargle periodogram in biological rhythm research: analysis of incomplete and unequally spaced time-series. *Biological Rhythm Research*. 1999; 30(2):178–201.

[11] Boardman A, Schlindwein FS, Rocha AP, Leite A. A study on the optimum order of autoregressive models for heart rate variability. *Physiological Measurement*. 2002;23(2):325.

[12] Burg JP. A new analysis technique for time series data. In: *Modern Spectrum Analysis*, edited by Childers DG. New York: IEEE Press. 1968;.

[13] Brennan M, Palaniswami M, Kamen P. Poincaré plot interpretation using a physiological model of HRV based on a network of oscillators. *American Journal of Physiology - Heart and Circulatory Physiology*. 2002; 283(5):H1873–H1886.

[14] Solem K, Laguna P, Sornmo L. An efficient method for handling ectopic beats using the heart timing signal. *Biomedical Engineering, IEEE Transactions on*. 2006; 53(1):13–20.

[15] Estévez M, Machado C, Leisman G, Estévez-Hernández T, Arias-Morales A, Machado A, Montes-Brown J. Spectral analysis of heart rate variability. *International Journal on Disability and Human Development*. 2016; 15(1):5–17.